

Effective Conductivity of a Suspension of Permeabilized Cells: A Theoretical Analysis

Mojca Pavlin and Damijan Miklavčič

University of Ljubljana, Faculty of Electrical Engineering, Ljubljana, Slovenia

ABSTRACT During the electroporation cell membrane undergoes structural changes, which increase the membrane conductivity and consequently lead to a change in effective conductivity of a cell suspension. To correlate microscopic membrane changes to macroscopic changes in conductivity of a suspension, we analyzed the effective conductivity theoretically, using two different approaches: numerically, using the finite elements method; and analytically, by using the equivalence principle. We derived the equation, which connects membrane conductivity with effective conductivity of the cell suspension. The changes in effective conductivity were analyzed for different parameters: cell volume fraction, membrane and medium conductivity, critical transmembrane potential, and cell orientation. In our analysis we used a tensor form of the effective conductivity, thus taking into account the anisotropic nature of the cell electroporation and rotation of the cells. To determine the effect of cell rotation, as questioned by some authors, the difference between conductivity of a cell suspension with normally distributed orientations and parallel orientation was also calculated, and determined to be <10%. The presented theory provides a theoretical basis for the analysis of measurements of the effective conductivity during electroporation.

INTRODUCTION

Research on the interaction of electric pulses and cells led to different biomedical applications. New methods such as electrofusion and electroporation are not only useful applications but can also reveal basic properties of cells and tissues. With the theories that explain dielectric and conductive properties of cell suspensions, we can interpret the experiments performed on a macroscopic level to obtain knowledge of biophysical processes on a microscopic level.

When an electric field is applied to a cell, a nonuniform transmembrane potential (TMP) is induced on the exposed cell. If the induced TMP is large enough, i.e., above the critical value (TMP_c), cell membrane becomes permeabilized in a reversible process called electroporation, thus allowing easier transport of ions and entrance of molecules that otherwise cannot easily cross the cell membrane (Neumann et al., 1982, 1989; Zimmermann, 1982; Weaver and Chizmadzhev, 1996; Jaroszeski et al., 1999; DeBruin and Krassowska, 1999a,b; Ryttsen et al., 2000). The value of TMP_c at the room temperature was reported to be between 0.2 and 1 V (Zimmermann, 1982, 1996; Tsong, 1991; Hibino et al., 1993; Teissie and Rols, 1993) depending also on the pulse parameters and experimental conditions (Miklavčič et al., 2000). Further increase of the electric field causes irreversible membrane permeabilization and cell death. Electroporation is of interest in a variety of applications specially for gene transfection, electrochemotherapy (Neumann et al., 1982; Sukharev et al., 1992; Jaroszeski et al., 1999; Mir, 2000; Serša et al., 2000), study of forces on

cells undergoing fusion (Zimmermann, 1982), and models of cardiac tissue response to defibrillating currents. With the development of the electroporation technique, theoretical aspects of the conductivity of cell suspensions are becoming of interest. Electroporation leads to the increase of the membrane permeability for ions and molecules; however, until now the mechanism of the electroporation has not been fully explained. The theory of electroporation assumes that induced TMP triggers the formation of structural changes in the membrane electropores (Zimmermann, 1982; Neumann et al., 1982; Weaver and Chizmadzhev, 1996). These changes in membrane cause increased membrane conductivity which consequently leads to a change in bulk conductivity, as has already been shown experimentally in cell suspensions (Kinosita and Tsong, 1979) and on cell pellets (Abidor et al., 1993, 1994). Indirectly, by measuring the transmembrane potential, changes in membrane conductivity of sea urchin eggs were also observed (Hibino et al., 1991). It was suggested that such an increase in bulk or tissue could be used for measuring in vivo the changes of the conductance of tissue due to permeabilization (Davalos et al., 2000, 2002).

Only a few studies have dealt with the calculation and measurement of the change in the effective conductivity. Abidor and co-authors (Abidor et al., 1993, 1994) measured changes of the resistance of cell pellets due to electroporation and the drop of the resistance was observed after the application of high-voltage pulses. Similarly, in another study (Kinosita and Tsong, 1979), authors observed an increase of the effective conductivity of suspension of erythrocytes with electric fields above 150 kV/m. These changes depended on the field strength, pulse duration, and conductivity of the extracellular medium. The conductivity of the suspension returned to its initial value after the pulses but increased again in the range of 10 s due to the diffusion of the ions from the cell. Authors estimated membrane conductance

Submitted April 13, 2002, and accepted for publication March 24, 2003.

Address reprint requests to Mojca Pavlin, M.Sc., University of Ljubljana, Faculty of Electrical Engineering, Tržaška 25, SI-1000 Ljubljana, Slovenia. Tel.: 386-1-476-8768; Fax: 386-1-426-4658; E-mail: mojca@svarun.fe.uni-lj.si.

© 2003 by the Biophysical Society

0006-3495/03/08/719/11 \$2.00

G_m to be between 10 S/cm^2 and 100 S/cm^2 . In these studies the effective conductivity was measured by impedance measurements, or by measuring current and voltage during high-voltage pulse or during measuring low voltage pulse applied after the high-voltage electroporative pulse. However, other authors (Zimmermann, 1982) questioned these results since the orientation of cells in dense suspensions was not taken into consideration. Indeed it was shown theoretically and confirmed experimentally (Zimmermann, 1982; Neumann et al., 1989) that a cell laying in an AC electric field starts to rotate in the presence of another cell due to the interaction with neighboring cells. Additionally, other mechanisms such as thermal relaxation and cell anisotropy cause cell rotation. Therefore, rotation also should be taken into account, especially in a dense suspension where many cells are interacting with each other.

In this article we present a theory, which describes how the effective (bulk) conductivity of a suspension of permeabilized cells depends on parameters such as a cell's volume fraction, conductivity of the medium, membrane conductivity, critical TMP, and cell orientation. We calculated the effective conductivity of a suspension of permeabilized cells by two different approaches: a numerical one by using a finite elements method (FEM), and an analytical one by using the equivalence principle. Both approaches include the anisotropic nature of the cell electroporabilization, and also takes into account the orientation of cells. With these two approaches it is thus possible to estimate the changes of the membrane conductivity from the measurements of the effective conductivity of a cell suspension.

METHODS

We analyzed the effective conductivity of a suspension of permeabilized cells analytically and numerically. Both approaches are connected with the equivalence principle and Maxwell equation as shown in Fig. 1. Maxwell equation is a mean-field approximation, which describes how the conductivity of one particle (cell) σ_p is connected with the effective conductivity σ of many particles dispersed in external medium. Since a biological cell is composed of different parts (membrane, cytoplasm, ...) having different specific conductivities we have to use the equivalence principle; this principle states that a nonhomogeneous particle in the electric field can be replaced with a sphere having the equivalent conductivity σ_p , neglecting higher than dipole terms. Therefore, analytically the equivalent conductivity of a single cell was obtained first, and then effective conductivity from Maxwell equation was obtained, whereas numerically we directly calculated the effective conductivity of a suspension and then the equivalent conductivity of a single cell was calculated.

As already mentioned, cells in suspension tend to rotate due to different forces. When cell is permeabilized, the conductivity becomes anisotropic (Fig. 1, left picture), so the orientation of the cell with respect to the electric field becomes important. For this reason the effect of a cell orientation on effective conductivity of a cell suspension was studied as well.

Numerical calculations

We built a finite-element model of a suspension of permeabilized cells. To model a homogeneous cell suspension, cells were organized into a simple-

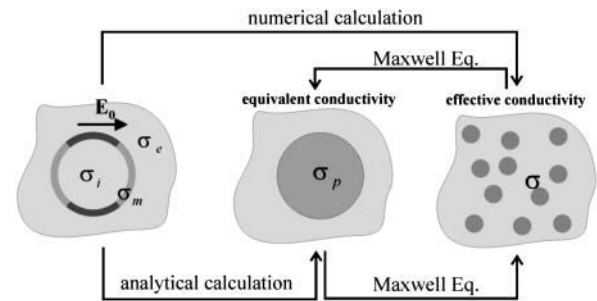


FIGURE 1 The two approaches, numerical and analytical, used to connect changes in membrane conductivity, σ_m , with changes of effective conductivity, σ . The equivalence principle enables us to replace a permeabilized cell with the anisotropic equivalent conductivity, σ_p , and the Maxwell equation connects conductivity of a single cell and effective conductivity of many cells.

cubic lattice, since we showed previously that the effective conductivity is similar for different cubic lattices (Pavlin et al., 2002b).

An idealized model of a biological cell is a sphere consisting of a cell cytoplasm σ_i surrounded by a very thin, low conducting membrane, σ_m^0 , which is placed in a conductive medium, σ_e . A model of a permeabilized cell is shown in Fig. 2. The brighter shaded part of the membrane represents the area of the membrane that has increased membrane conductivity, σ_m , and θ_c denotes the critical angle of electroporation, where the induced TMP exceeds the critical value TMP_c .

It was shown experimentally (Gabriel and Teissie, 1998) that parameter θ_c depends on the applied electric field according to equation: $TMP_c = 3/2 E_0 R \cos \theta_c$, while the conductivity of the permeabilized area, σ_m , depends both on electric field strength and on pulse duration (Hibino et al., 1993). In our models permeabilization is assumed to be symmetrical on both poles although some conductance asymmetry was observed (Hibino et al., 1993). We did not include this effect in our models since large asymmetry in permeabilization which was assumed by some authors to be due to the resting potential (Zimmerman, 1982; Tekle et al., 1990; Gabriel and Teissie, 1997) occurs only very near the TMP_c (DeBruin and Krassowska, 1999a,b; Valič et al., 2003).

The thickness of a cell membrane for a typical cell having $R = 10 \mu\text{m}$ is $d = 5 \text{ nm}$, a factor of 2000 smaller than the cell radius. Due to the limited computer capabilities, the realistic cell was approximated with one having an

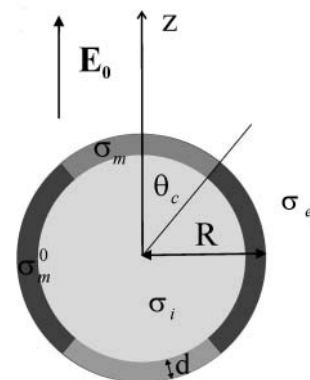


FIGURE 2 The FEM model of a permeabilized cell for parallel orientation. Brighter shaded part of membrane represents the area of the membrane with increased membrane conductivity; (σ_m , θ_c) denotes the critical angle of electroporation.

unrealistic membrane thickness $d' = 0.5 \mu\text{m}$ and correspondingly higher membrane conductivity:

$$\sigma'_m = \frac{d'}{d} \sigma_m, \quad (1)$$

where σ_m is membrane conductivity at the permeabilized pole cap and σ'_m is the scaled membrane conductivity. This approximation is valid under the assumption that we are interested only in the effective conductivity and not in the electric field inside the membrane. We verified this approximation by building a model, which had thickness d' of $10\times$ smaller, but we did not observe any change in the effective conductivity. We calculated models for four different membrane conductivities of the permeabilized area, $\sigma_m = 1 \times 10^{-5} \text{ S/m}$, $1 \times 10^{-4} \text{ S/m}$, $2 \times 10^{-4} \text{ S/m}$, and $4 \times 10^{-4} \text{ S/m}$, and two critical angles, $\theta_c = 30^\circ$ and 45° . The values of membrane conductivity except for the lowest were chosen in range as given in Hibino et al. (1991), where the potential distribution obtained with fluorescent imaging of permeabilized sea urchin eggs corresponded to the membrane conductance G_m between 1.8 S/cm^2 and 4.3 S/cm^2 . Because membrane conductivity after the pulses rapidly decreases due to resealing (Hibino et al., 1991, 1993) also one order smaller value of membrane conductance $G_m = 0.2 \text{ S/cm}^2$ ($\sigma_m = 10^{-5} \text{ S/m}$) was used. For the cytoplasm conductivity we used the value reported in literature (Foster and Schwan, 1986) $\sigma_i = 0.5 \text{ S/m}$. The choice of the external medium is arbitrary, since it does not affect the cell equivalent conductivity; therefore we chose the case where the external conductivity is equal to the internal ($\sigma_e = \sigma_i = 0.5 \text{ S/m}$). We verified this (results not shown) by calculating the effective conductivity for lower value ($\sigma_e = 0.123 \text{ S/m}$) and obtained same results.

To study the effect of the cell orientation on the effective conductivity of a cell suspension, we modeled three extreme cases of orientations, with all cells having their principal axis z' oriented by angles: $\vartheta = 0^\circ$, 45° , and 90° with respect to the external field.

Using the symmetry of a cubic lattice and applying appropriate boundary conditions we were able to model an infinite cubic lattice with a model of a unit lattice cell (the part of the lattice which contains the symmetry of the lattice; see Susil et al., 1998; Pavlin et al., 2002a). In all our models, voltage V was applied on the face normal to z -axis. Varying A , the length of the unit cell side, calculations were performed for three cell volume fractions: $f = 0.1$, $f = 0.15$, and $f = 0.3$, where $f = 4\pi/3(R/A)^3$. Numerical calculations were performed by a commercial finite element modeling software EMAS (Ansoft, Pittsburgh, PA). Details of this program and FEM method are described elsewhere (Šemrov and Miklavčič, 1999). The static current flow analysis was chosen to calculate the current density distribution and the effective conductivity was obtained using Ohm's law: $\sigma = j/E$.

Analytical calculations—effective medium theory

The exact calculation of the effective (bulk) conductivity of a cell suspension is theoretically a complex problem especially due to mutual interactions among the cells. Effective medium theories use average field and neglect local field effects (Dukhin, 1971; Takashima, 1989) to obtain approximate analytical solutions. For the effective conductivity σ of a dilute suspension, Maxwell obtained (Maxwell, 1873; Takashima, 1989)

$$\frac{\sigma_e - \sigma}{2\sigma_e + \sigma} = f \frac{\sigma_e - \sigma_p}{2\sigma_e + \sigma_p}, \quad f = \frac{NV_c}{V}, \quad (2)$$

where σ_p is the conductivity of the particle, σ_e the conductivity of the external medium, and f is the volume fraction of the particles dispersed in the medium. Maxwell's derivation is based on the assumption that the potential of N spheres is equal to the potential of a sphere having the effective conductivity σ . Maxwell's equation is exact in the first order of f , hence for dilute suspensions. However, it was experimentally (Foster and Schwan, 1986) and numerically shown (Pavlin et al., 2002a) that Maxwell's approximation holds well also for higher volume fractions; i.e., denser suspensions.

Maxwell's equation can be used to calculate the effective conductivity of a cell suspension if we replace the cell which is a heterogeneous structure having membrane conductivity σ_m and interior σ_i with a homogeneous sphere having the equivalent conductivity σ_p (Pauly and Schwan, 1959; Dukhin, 1971):

$$\sigma_p = \sigma_m \frac{2(1 - \nu)\sigma_m + (1 + 2\nu)\sigma_i}{(2 + \nu)\sigma_m + (1 - \nu)\sigma_i} \quad \nu = (1 - d/R)^3. \quad (3)$$

This equation holds for the case when membrane thickness, d , is much smaller than the cell radius, R , which is valid for biological cells. The exact solution and more complex expression was first derived by Pauly and Schwan (1959). From Eq. 3 one can obtain the equivalent conductivity of a nonpermeabilized cell which is $\sigma_p = 2 \times 10^{-4} \text{ S/m}$ for physiological values of parameters ($\sigma_m = 10^{-7} \text{ S/m}$, $\sigma_i = 0.5 \text{ S/m}$). Thus, for normal physiological conditions ($\sigma_e = 1.2 \text{ S/m}$), cells are practically nonconductive. This, however, is not true for low ($\sigma_e < 0.01 \text{ S/m}$) conducting mediums (Kotnik et al., 1997).

In the case of electroporation, the increase in membrane conductivity due to the membrane "pores" causes an increase of the cell equivalent conductivity. The nonuniform induced TMP leads to a nonuniform increase of membrane conductance (where induced $TMP > TMP_c$) and consequently to anisotropic equivalent conductivity of a cell σ_p which can be described as a diagonal tensor in the coordinate system where the z' -axis is the axis of the symmetry of a permeabilized cell:

$$\sigma'_p = \begin{bmatrix} \sigma_{\perp} & 0 & 0 \\ 0 & \sigma_{\perp} & 0 \\ 0 & 0 & \sigma_{\parallel} \end{bmatrix}. \quad (4)$$

The diagonal elements σ_{\parallel} and σ_{\perp} represent values of conductivity when electric field is parallel or perpendicular to z' . Thus the effective conductivity of a cell suspension also becomes anisotropic. In the above definition of σ_p , we assume that even though membrane has locally increased membrane conductivity at the pole caps, a cell can still be replaced with the equivalent conductivity. This is an approximation which takes into account only the change in the dipole term of the electric field and not higher terms as shown later on in the analytical derivation of σ_p .

When electric field is applied, a cell is permeabilized on pole caps so that at the start of the electroporative pulse all cells are oriented parallel to electric field as shown in Fig. 2. But due to different mechanisms (AC field, interactions, and cell nonhomogeneity) cells in a suspension start to rotate. Therefore, due to anisotropic nature of permeabilization and rotation of cells we have to consider tissue or suspension of cells as a nonhomogeneous anisotropic material. In this article we use, unlike in previous approaches, the anisotropic version of the Maxwell equation (Levy and Stroud, 1997) for the calculation of the effective conductivity of the mixture of anisotropic cells dispersed in an isotropic medium. The solution derived in Appendix A gives the tensor of the effective conductivity depending on the orientation distribution of the cells over angles ϑ and ϕ where ϑ is the angle between the principal conductivity axis and the external electric field and the angle ϕ is the angle of rotation of a cell around the z -axis. In the case where all cells are oriented parallel to the electric field ($z' \parallel z$) the tensor of the effective conductivity is diagonal; i.e., $\sigma_{i \neq j} = 0$ and diagonal elements are (Eq. A9):

$$\begin{aligned} \sigma_{11} = \sigma_{22} &= \sigma_e + 3f\sigma_e \frac{(\sigma_{\perp} - \sigma_e)}{(\sigma_{\perp} - \sigma_e)(1 - f) + 3\sigma_e}, \\ \sigma_{33} &= \sigma_e + 3f\sigma_e \frac{(\sigma_{\parallel} - \sigma_e)}{(\sigma_{\parallel} - \sigma_e)(1 - f) + 3\sigma_e}. \end{aligned} \quad (5)$$

Thus the generalized equation reduces to Maxwell equation when replacing σ_p with σ_{\parallel} for parallel orientation and σ_p with σ_{\perp} for perpendicular orientation.

For cells in a suspension we can assume that all cells are first oriented in the direction of the applied field since permeabilization occurs at the pole caps of a cell. But due to different forces, a cell in a suspension starts to

rotate so we can assume normal distribution of the angles ϑ around angle $\vartheta = 0$ ($z = 1$) and a uniform distribution over ϕ :

$$\Gamma(z) = \frac{1}{\gamma\sqrt{2\pi}} e^{-(z-1)^2/2\gamma^2}, \quad (6)$$

where $z = \cos \vartheta$ and γ is the width of the distribution. From this, we obtain (derivation is given in Appendix A) the effective conductivity in the direction of the applied field:

$$\sigma_{33} = \sigma_e + 3f\sigma_e \frac{A_{33}}{(1-f)(\sigma_{\perp} + 2\sigma_e)(\sigma_{\parallel} + 2\sigma_e) + 3f\sigma_e B_{33}}, \quad (7)$$

where A_{33} and B_{33} are components of the two matrices A and B given in Eq. A15. This result (Eq. 7) directly applies when conductivity after the pulse is measured with a second low voltage pulse. However, if cells rotate during the pulse, then permeabilized area changes and for this particular case equivalent conductivity should be calculated for larger critical angle. Nevertheless, calculation of the effective conductivity from equivalent conductivity is the same as derived above.

Analytical calculations—equivalent conductivity of a permeabilized cell

In this section we derive an equation which connects cell properties of a permeabilized cell with the macroscopic effective conductivity of the cell suspension. We start with the solution of Laplace's equation for a model of a permeabilized cell oriented in the direction of the applied field (Fig. 2) following the calculations of Hibino et al. (1991). All calculations apply to an isolated cell so that the interactions between the cells are neglected. It was shown numerically (Pavlin et al., 2002b) that for volume fractions from 0.1 to 0.5, the changes of TMP due to the cell-to-cell interactions are in a range from 5% to 17%.

For a function $g(\theta)$ which describes the membrane conductivity, we assumed that the membrane permeability has a nonzero value for absolute values of angles under critical angle and zero elsewhere,

$$g(\cos \theta) = \begin{cases} g_0 \frac{(|\cos \theta| - \cos \theta_c)^j}{(1 - \cos \theta_c)^j} & |\cos \theta| > \cos \theta_c \\ 0 & |\cos \theta| \leq \cos \theta_c \end{cases}, \quad (8)$$

where g_0 is the normalized maximal membrane conductance at the two poles of the cell,

$$g_0 = \frac{\sigma_m R}{\sigma_i d}, \quad \nu = \frac{\sigma_i}{\sigma_e}. \quad (9)$$

The parameter j represents functional dependency of the membrane conductance on the induced TMP. For $j = 0$ the membrane conductivity for the angles under the critical value is constant, and for $j = 1$ we assume that the conductivity of the permeabilized area is linearly proportional to the induced TMP. Experiments in which the authors (Gabriel and Teissie, 1998) used rapid fluorescent imaging to measure cell permeabilization indicate that membrane conductivity is constant in the area above the TMP_c . In our calculations we used $j = 0$ and $j = 1$ even though this procedure allows other functional dependencies of $g(\theta)$ ($j > 0$).

In Appendix B, we derive the potential of a permeabilized cell which is oriented in the direction of the applied external electric field for a given value of θ_c , g_0 , and ν ,

$$\Psi_i = c_0 + \sum_{n=1}^{\infty} \frac{c_n (r')^n P_n(\cos \theta)}{n},$$

$$\Psi_e = \left[r' + \frac{1}{2r'^2} \right] P_1(\cos \theta) + \nu \sum_{n=1}^{\infty} \frac{c_n P_n(\cos \theta)}{(n+1)(r')^{n+1}}, \quad (10)$$

where the P_n values are the Legendre polynomials. The c_n coefficients are calculated for finite number $n = N$, thus reducing an infinite system of equations to a finite one. For high enough N (in our case $N = 30$), we get negligible error resulting from this approximation. Eq. 10 is an analytical solution for the induced potential of a permeabilized cell in external electric field from which the induced TMP can be obtained

$$TMP/E_0 R = \Psi_e(R) - \Psi_i(R). \quad (11)$$

In Fig. 3 the dependence of the induced TMP on the angle θ and the parameter g_0 (maximum membrane conductivity) is shown. Fig. 3 can be interpreted in the following way: when the induced TMP reaches the critical value (TMP_c), the membrane is permeabilized and starts to conduct ionic current. The membrane conductivity immediately rises to a level which is sufficient to keep the TMP below the critical value ($g_0 > 0.4$). By fitting experimental data of fluorescent imaging to this mathematical model, Hibino and co-workers (Hibino et al., 1991, 1993) determined the values of g_0 , and by this, of σ_m .

Up to now we have assumed that θ_c is constant. One possibility is also that θ_c and with this the area of permeabilization could expand during the pulse. Even though this was not observed for transport of large molecules where θ_c did not change (Gabriel and Teissie, 1997), we still have to consider θ_c as an average value, which determines the area through which the transport of ions occurs.

We used the solution of Laplace equation to derive an equation for the equivalent conductivity of a permeabilized cell. Similarly as in deriving the Maxwell equation, we assume that potential of permeabilized cell Ψ_e given in Eq. 10 is equal to the potential of an equivalent sphere having the conductivity σ_p , and hence,

$$\Psi_e = \left[r' + \frac{1}{2r'^2} \right] P_1(\cos \theta) + \nu \sum_{n=1}^{\infty} \frac{c_n P_n(\cos \theta)}{(n+1)(r')^{n+1}} \simeq \Psi_{eq}$$

$$= \left[r' + \frac{\sigma_e - \sigma_p}{2\sigma_e + \sigma_p} \frac{1}{r'^2} \right] P_1(\cos \theta). \quad (12)$$

Neglecting higher multipole terms, we obtain the following equation for σ_p and the effective conductivity σ :

$$\frac{1}{2}(1 - \nu c_1) = \frac{\sigma_e - \sigma_p}{2\sigma_e + \sigma_p} = \frac{1}{f} \frac{\sigma_e - \sigma}{2\sigma_e + \sigma}, \quad (13)$$

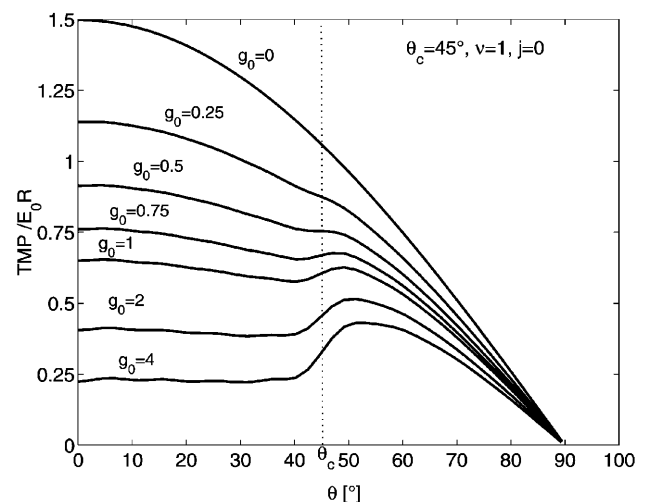


FIGURE 3 Dependence of the induced TMP on the angle θ and the parameter g_0 (membrane conductivity) for $\nu = \sigma_i/\sigma_e = 1$, $\theta_c = 45^\circ$, and $j = 0$. TMP is normalized to electric field E_0 and radius of the cell R . For $g_0 = 0$, we obtain the static Schwan equation, $TMP/E_0 R = \cos \theta$.

where c_1 is the dipole term from the Eq. 10 and $\nu = \sigma_j/\sigma_e$. Eq. 13 is an analytical solution that connects membrane conductivity with the effective conductivity of many cells. In this equation, $\sigma_p = \sigma_{||}$, since the cell is oriented in the direction of the electric field. To obtain σ_{\perp} the derivation should be extended for perpendicular orientation using series expansion with Legendre polynomials and spherical functions; however, all the procedure is analogous as for $\sigma_{||}$. Eq. 13 uses a dipole approximation since it neglects higher multipole terms. It directly connects membrane conductivity with the equivalent conductivity of a cell and via Maxwell's equation with the effective conductivity of a cell suspension. With Eq. 13 it is thus possible to calculate the effective conductivity of a cell suspension for given f , σ_m , σ_i , σ_e , and θ_c ; and vice versa, the membrane conductivity from the effective conductivity of a cell suspension.

RESULTS

We calculated the effective conductivity of a suspension of permeabilized cells numerically by using a FEM method and analytically by using equivalence principle. Analytically we first calculated the component of the equivalent conductivity of a permeabilized cell for parallel orientation, $\sigma_{||}$, from which the effective conductivity σ of a cell suspension can be obtained. With FEM method, however, we directly calculated the effective conductivity, and then using the Maxwell equation, we obtained the equivalent conductivity as shown in Fig. 1.

In Table 1 we compare the results for cell equivalent conductivity $\sigma_{||}$ calculated analytically with Eq. 13 and numerically for given θ_c and σ_m . In our numerical study, we calculated models of cell suspension of three different volume fractions of cells: $f = 0.1$, $f = 0.15$, and $f = 0.3$. From the FEM result for the effective conductivity, σ/σ_e , we obtained the equivalent conductivity using the Maxwell equation (Eq. 2). Since $\sigma_{||}$ depends only on cell parameters and not on the volume fraction, the differences are due to dipole approximation and numerical error. Therefore, the numerical results for the three volume fractions were averaged to obtain $\langle\sigma_{||}\rangle$ for comparison with analytical calculations and we can see that the analytical results are in good agreement with the numerical results. Both approaches use dipole approximation; therefore, they are exact in the first order of f . In Table 1 we also compare the analytical results for the case where conductivity of the permeabilized area is

constant ($j = 0$) and proportional to the induced TMP ($j = 1$), and we can observe that there is no significant difference in the equivalent conductivity.

In Fig. 4, the results for normalized effective conductivity, σ/σ_e , of the FEM models (*symbols*) are compared to σ/σ_e ($\sigma_e = 0.5$ S/m) calculated with Maxwell's equation (*lines*) for the analytical values of $\sigma_{||}$ for parameters σ_m and θ_c given in Table 1. Again, it can be seen that the FEM results for the equivalent conductivity $\sigma_{||}$ are in good agreement with the analytical results, which means that a permeabilized cell can be replaced with a sphere having the equivalent conductivity calculated using Eq. 13.

Effect of different parameters on the effective conductivity of a cell suspension

We further investigated how the relative change in the effective conductivity depends on the cell permeabilization parameters. Fig. 5, *a* and *b*, summarize how the relative change of conductivity $((\sigma - \sigma_0)/\sigma_0)$ depends on the volume fraction (f), membrane conductance (σ_m), critical angle (θ_c), and conductivities of the external and the internal medium (*a*) $\sigma_e = 0.5\sigma_i$ and (*b*) $\sigma_e = 2\sigma_i$, where σ_0 is the initial effective conductivity of a cell suspension before electro-permeabilization, $\sigma_0 = \sigma$ ($\sigma_m = 0$).

As expected, the relative change of the effective conductivity is larger for higher volume fractions and higher membrane conductivity. It can be also seen that when the membrane conductivity drops for one order of magnitude, for example, due to resealing, the relative change of the effective conductivity for $f < 0.3$ is $< 5\%$, which means that very quickly after the end of a pulse the conductivity of a cell suspension drops to the initial value, which also agrees with what was experimentally observed (Abidor et al., 1993; Hibino et al., 1993).

The comparison of Fig. 5, *a* and *b*, shows that ratio of σ_e/σ_i also changes the results significantly, and that for low conductive medium the changes in relative conductivity are more pronounced. However, in such a case, when $\sigma_e < \sigma_i$, one has to consider also the effect of the leakage of the ions from the cell as shown in Kinoshita and Tsong (1979), and its

TABLE 1 Comparison of the analytical results for the equivalent cell conductivities, σ_p , for the parallel orientation, $\sigma_{||}$, with the numerical results for the calculated parameters

$R = 10 \mu\text{m}$, $d' = 0.5 \mu\text{m}$, $\sigma_i = 0.5 \text{ S/m}$	FEM $\sigma_{ }$ S/m ($f = 0.1$)	FEM $\sigma_{ }$ S/m ($f = 0.15$)	FEM $\sigma_{ }$ S/m ($f = 0.3$)	FEM* $\langle\sigma_{ }\rangle$ S/m	Analyt. [†] $\sigma_{ }$ S/m $j = 0$	Analyt. [†] $\sigma_{ }$ S/m $j = 1$
$\theta_c = 30^\circ$ $\sigma_m = 1 \times 10^{-5}$ S/m	0.007	0.012	0.006	0.008	0.005	0.007
$\theta_c = 45^\circ$ $\sigma_m = 1 \times 10^{-5}$ S/m	0.012	0.012	0.015	0.013	0.012	0.013
$\theta_c = 30^\circ$ $\sigma_m = 1 \times 10^{-4}$ S/m	0.054	0.060	0.054	0.056	0.056	0.056
$\theta_c = 45^\circ$ $\sigma_m = 1 \times 10^{-4}$ S/m	0.094	0.099	0.094	0.096	0.098	0.100
$\theta_c = 30^\circ$ $\sigma_m = 2 \times 10^{-4}$ S/m	0.090	0.088	0.084	0.087	0.093	0.093
$\theta_c = 45^\circ$ $\sigma_m = 2 \times 10^{-4}$ S/m	0.152	0.151	0.151	0.151	0.157	0.155
$\theta_c = 30^\circ$ $\sigma_m = 4 \times 10^{-4}$ S/m	0.135	0.133	0.128	0.132	0.134	0.139
$\theta_c = 45^\circ$ $\sigma_m = 4 \times 10^{-4}$ S/m	0.219	0.219	0.218	0.219	0.226	0.216

* $\langle\sigma_{||}\rangle = 1/3[\sigma_{||}(f = 0.1) + \sigma_{||}(f = 0.15) + \sigma_{||}(f = 0.3)]$.

[†]Calculated with Eq. 13.

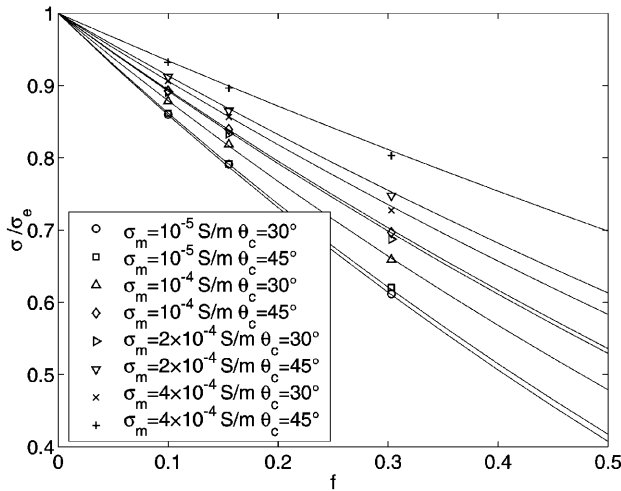


FIGURE 4 The results for normalized effective conductivity σ/σ_c of the FEM models (symbols) are compared to the analytical results (lines) for a case of a parallel orientation ($\vartheta = 0$). Each line represents the effective conductivity calculated from the theoretical value of σ_p using Eq. 13, which we derived analytically.

contribution to the increased bulk conductivity especially for low conductive media. Nevertheless, time constant for diffusion of ions (milliseconds) is usually longer than the pulse duration ($10 \mu\text{s} - 1 \text{ ms}$) so that diffusion can be neglected in the case of relatively short pulses.

Effect of cell orientation on the effective conductivity of a cell suspension

Up to now, we assumed that all cells are oriented with the axis of symmetry parallel to the external electrical field, since, during a DC pulse and low frequency AC pulses, this is the orientation having the minimum free energy, and is thus the stable orientation. The orientation of cells in the electric field can change either due to cell rotation caused by the forces, which act on a cell in a suspension, or due to the change of electric field orientation by using different electrodes. For this reason we calculated the effective conductivity using the generalized Maxwell equation given in the theoretical section for a given orientation distribution. In the special case of a random orientation distribution, the effective conductivity is a scalar given by Eq. A10. For the extreme case where all cells are oriented perpendicular to the external electrical field ($\sigma = \sigma_{11}$), we obtained 10–20% decrease of the effective conductivity compared to the parallel orientation ($\sigma = \sigma_{33}$), and for the values for random orientation, we obtained that the effective conductivity is approximately $\sigma = (\sigma_{11} + \sigma_{33})/2$.

However, after the pulse cells start to rotate due to different relaxation mechanisms and forces, for this case we therefore assumed normal distribution over the angles ϑ around angle $\vartheta = 0$ as defined in Eq. 6. Normal distribution is a good approximation in a case of many collaborating

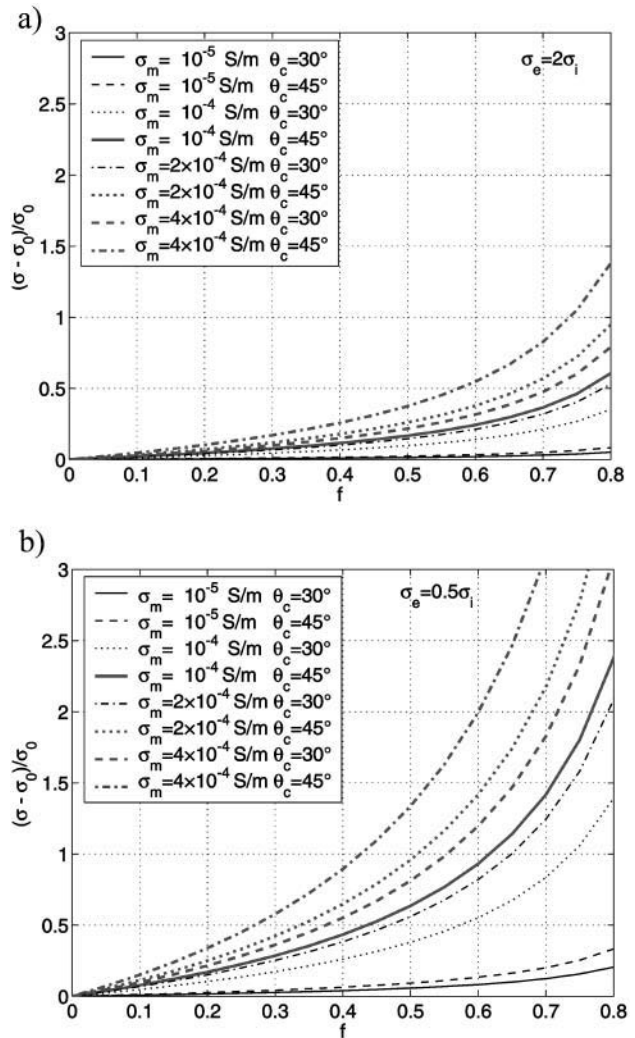


FIGURE 5 The relative change of conductivity, $(\sigma - \sigma_0)/\sigma_0$, is plotted against cell volume fraction for (a) $\sigma_c = 0.5\sigma_i$ and (b) $\sigma_c = 2\sigma_i$ for different membrane conductivities and critical angles, where σ_0 is initial conductivity of a suspension of cells before electroporation ($\sigma_0 = \sigma(\sigma_m = 0)$).

processes where all distributions limit to normal distribution. In Fig. 6 the effective conductivity in the direction of the applied field (σ_{33}) is calculated for different volume fractions with Eq. 7. For $\gamma = 0.5$ (majority of cell orientations are between $\vartheta = -\pi/3$ and $\vartheta = \pi/3$), we obtained, using Eq. 7, the drop of the effective conductivity for $\sim 10\%$. Thus, this effect can be neglected.

We have to stress that this applies only for the case when the second pulse is a low-voltage measuring pulse. If the second pulse is above the threshold value for permeabilization, additional area is permeabilized that is not considered in our calculations.

DISCUSSION AND CONCLUSIONS

The objective of our work was to calculate the effective (bulk) conductivity of a cell suspension for different pa-

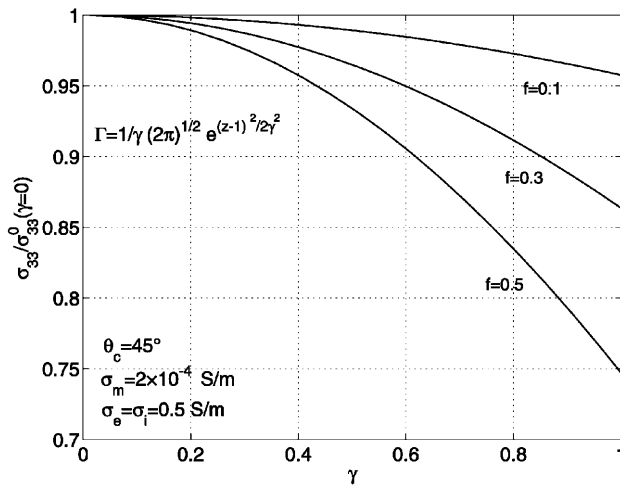


FIGURE 6 Effect of cell rotation around parallel orientation. Effective conductivity in the direction of the applied field, σ_{33} , is calculated with Eq. 7 for a uniform distribution of angles ϕ and normal distribution (Eq. 6) of the angles ϑ around angle $\vartheta = 0$ ($z = 1$), $z = \cos \vartheta$. Here, γ is the width of the distribution, and σ_{33}^0 is the effective conductivity when all cells are oriented parallel to the applied electric field, $\sigma_{33}^0 = \sigma_{33}(\gamma = 0)$.

rameters: cell volume fraction, membrane conductivity, cytoplasm and medium conductivity, critical transmembrane potential (critical angle), and cell orientation by taking into account also the “anisotropic” nature of membrane permeabilization. We pursued this objective by choosing two different approaches: a numerical and an analytical one. Both consider a permeabilized cell as a particle having anisotropic conductivity. Using the analytical solution for the potential of a permeabilized cell in an electric field, we derived the equation for the equivalent conductivity of the cell using the equivalence principle. Then the effective conductivity of a cell suspension was calculated using a generalized Maxwell’s equation, whereas numerically, the effective conductivity was calculated directly. The comparison of numerical and analytical calculations showed good agreement, which means that a permeabilized cell can be replaced with a sphere having the equivalent conductivity as derived in Eq. 13.

We analyzed how the relative change of the effective conductivity $(\sigma - \sigma_0)/\sigma_0$ depends on the cell volume fraction, f ; membrane conductivity, σ_m ; critical angle, θ_c ; and conductivities of the external medium and cytoplasm, σ_e and σ_i , respectively. We showed that relative changes of the effective conductivity strongly depend on the value of the external conductivity. For the membrane conductivities being $1 \times 10^{-4} - 4 \times 10^{-4}$ S/m and for volume fractions being typically 0.05–0.4, the relative change $(\sigma - \sigma_0)/\sigma_0$ is between 5% and 30%.

Furthermore, the effect of cell orientation on the effective conductivity of a cell suspension was analyzed, which was not studied in previous reports. Using generalized Maxwell theory for the effective conductivity of anisotropic particles

that can rotate, we calculated the results for the limiting cases: parallel, perpendicular, and random orientation.

For cells in a suspension, we assumed that during a DC pulse they are preferentially oriented in the most stable position which is the parallel orientation. For this reason, we calculated the effective conductivity after the pulse, using a normal distribution over angles ϑ around $\vartheta = 0$. By this we evaluated that for cells in a suspension, the effective conductivity calculated for parallel orientation is decreased <10% due to cell rotation after the pulse.

In our theoretical analysis we used several limitations. Calculations were performed only for spherical shape of cells even though a lot of cells, such as erythrocytes, bacteria, . . . , are not spherical. However, FEM calculations can be extended also for the calculation of the effective conductivity of a suspension of spheroidal cells or even cells of irregular shapes. We also calculated the difference in relative change of the effective conductivity due to the shape of ellipsoidal cells (results not shown here) and obtained that, for ellipsoidal cells having ratio between the two radii >0.9, the difference is <2%.

We have limited our calculations to a DC case, which holds also for the frequencies under the relaxation frequency, which is ~ 1 MHz for low-conductive membranes. However, both the analytical and numerical calculation can also be extended to a general AC case by using generalized conductivity, which also takes into account dielectric properties (Pavlin et al., 2002a).

The presented analysis directly applies for a cell suspension; therefore, we limited numerical calculations to volume fractions of 0.3, which corresponds to a dense suspension. We did not extend our numerical calculations to higher volume fractions, since for an FEM model of a tissue it would be important to include specific geometry of cells and other structures of a specific tissue, which is beyond the scope of this article. However, because it was shown that the Maxwell equation is also valid for dense suspensions, we can calculate the effective conductivity for higher volume fractions, as presented in Fig. 5.

Both analytical and numerical calculations are based on the concept of equivalency and are thus approximate. We made approximations on two different levels. First, the electric field of a permeabilized cell laying in the external field is a multipole field, and therefore the equivalence principle is an approximation also for an isolated cell since we neglect higher multipoles terms (c_n values). Second, in a many-particle system such as a cell suspension, an electric field is a sum of multipole fields, and thus Maxwell’s equation is exact only in the first order of f (for dilute suspensions). However, in previous studies it was shown that Maxwell’s equation is also a good approximation for higher volume fractions (Foster and Schwan, 1986) and increased membrane conductivity (Pavlin et al., 2002a). By comparing the analytical results to numerical results, we conclude that the Maxwell equation can also be used for the calculation of

the effective conductivity of a suspension of permeabilized cells.

By considering normal distribution of orientations of cells in a suspension, we showed that rotation of cells due to different relaxation mechanisms decreases the effective conductivity only to a smaller extent for DC fields for the case where a second low voltage pulse is applied. In general the theory can be applied for any given orientation distribution and also for cells in tissue where electric field orientation is changed. Thus, providing that the TMP_c , and by this, θ_c , is defined, our theory provides a tool to estimate the changes in membrane conductivity based on the measurements of bulk effective conductivity of permeabilized cells.

Unlike previous approaches, where the electric cell properties were considered as isotropic scalar quantities, our model introduces the effective cell conductivity as a tensor that also takes into account the nonuniform electroporation of the cell membrane. Although the theoretical analysis presented in the article directly applies to cell suspensions in a DC field, it can readily be extended to more concentrated cell samples or tissues in DC or alternating fields. Thus it provides a theoretical basis for the analysis of measurements of the effective conductivity during electroporation which could be used as a way to online monitoring of cell permeabilization.

$$\sigma_p = \mathbf{M}_{\vartheta, \phi} \sigma'_p \mathbf{M}_{\vartheta, \phi}^T, \quad (\text{A1})$$

where $\mathbf{M}_{\vartheta, \phi}$ represents the matrix of rotation of a given cell (in general defined by the three Euler angles), and σ'_p is a diagonal tensor in a coordinate system defined by conductivity axis. For a uniaxial symmetrically permeabilized cell, where a cell has one conductivity value along the direction of the field and the other in the perpendicular direction, the equivalent conductivity writes as

$$\sigma'_p = \begin{pmatrix} \sigma_{\perp} & 0 & 0 \\ 0 & \sigma_{\perp} & 0 \\ 0 & 0 & \sigma_{\parallel} \end{pmatrix}. \quad (\text{A2})$$

A generalized tensor form of Maxwell theory can be derived which gives for the bulk effective conductivity tensor

$$\sigma = \sigma_e \mathbf{I} + 3f \sigma_e \left\langle \frac{\sigma_p - \sigma_e \mathbf{I}}{\sigma_p + 2\sigma_e \mathbf{I}} \right\rangle_{\mathbf{M}} \times \frac{1}{(1-f) + 3f \sigma_e \langle (\sigma_p + 2\sigma_e \mathbf{I})^{-1} \rangle_{\mathbf{M}}} \mathbf{E}_0, \quad (\text{A3})$$

where $\langle \rangle_{\mathbf{M}}$ denotes an average over the conductivity tensor orientation of each cell. Eq. A3 is the Maxwell result for mixtures of anisotropic particles.

For a mixture of such particles (cells) embedded in an isotropic medium, it is convenient to define such a coordinate system that \mathbf{E} is applied in the positive z -direction. The rotation matrix \mathbf{M} then depends only on two orientation angles: ϑ and ϕ between the principal conductivity axes and the z -axes. In this coordinate system, the conductivity tensor of each cell can be written as

$$\sigma_p = \sigma_{\perp} \mathbf{I} + a \begin{pmatrix} \cos^2 \phi \sin^2 \vartheta & \cos \phi \sin \phi \sin^2 \vartheta & \cos \phi \cos \vartheta \sin \vartheta \\ \cos \phi \sin \phi \sin^2 \vartheta & \sin^2 \phi \sin^2 \vartheta & \sin \phi \cos \vartheta \sin \vartheta \\ \cos \phi \cos \vartheta \sin \vartheta & \sin \phi \cos \vartheta \sin \vartheta & \cos^2 \vartheta \end{pmatrix}, \quad (\text{A4})$$

APPENDIX A

Here we present derivation of generalized Maxwell theory for calculation of the effective conductivity for mixture of anisotropic particles dispersed in

where $a = \sigma_{\parallel} - \sigma_{\perp}$. By defining $b = (\sigma_{\perp} + 2\sigma_e)(\sigma_{\parallel} - \sigma_e)$, the explicit expression for the bulk effective conductivity can be obtained as

$$\sigma = \sigma_e \mathbf{I} + \frac{3f \sigma_e A}{(\sigma_{\perp} + 2\sigma_e)(\sigma_{\parallel} + 2\sigma_e)} \left[1 - f + \frac{3f \sigma_e B}{(\sigma_{\perp} + 2\sigma_e)(\sigma_{\parallel} + 2\sigma_e)} \right]^{-1}, \quad (\text{A5})$$

where

$$A = \begin{pmatrix} b - 3a\sigma_e \langle \cos^2 \vartheta + \sin^2 \phi \sin^2 \vartheta \rangle & \frac{3a\sigma_e}{2} \langle \sin 2\phi \sin^2 \vartheta \rangle & \frac{3a\sigma_e}{2} \langle \cos \phi \sin 2\vartheta \rangle \\ \frac{3a\sigma_e}{2} \langle \sin 2\phi \sin^2 \vartheta \rangle & b - 3a\sigma_e \langle \cos^2 \vartheta + \cos^2 \phi \sin^2 \vartheta \rangle & \frac{3a\sigma_e}{2} \langle \sin \phi \sin 2\vartheta \rangle \\ \frac{3a\sigma_e}{2} \langle \cos \phi \sin 2\vartheta \rangle & \frac{3a\sigma_e}{2} \langle \sin \phi \sin 2\vartheta \rangle & b + \frac{3a\sigma_e}{2} (\langle \cos 2\vartheta \rangle - 1) \end{pmatrix}, \quad (\text{A6})$$

isotropic medium (Levy and Stroud, 1997). We assume that a permeabilized cell has an anisotropic conductivity, which is defined as a tensor σ_p . Every cell is oriented differently so that

and

$$B = \begin{pmatrix} \sigma_{\perp} + 2\sigma_{\parallel} + a\langle \cos^2 \vartheta + \sin^2 \phi \sin^2 \vartheta \rangle & -\frac{a}{2}\langle \sin 2\phi \sin^2 \vartheta \rangle & -\frac{a}{2}\langle \cos \phi \sin 2\vartheta \rangle \\ -\frac{a}{2}\langle \sin 2\phi \sin^2 \vartheta \rangle & \sigma_{\perp} + 2\sigma_{\parallel} + a\langle \cos^2 \vartheta + \cos^2 \phi \sin^2 \vartheta \rangle & -\frac{a}{2}\langle \sin \phi \sin 2\vartheta \rangle \\ -\frac{a}{2}\langle \cos \phi \sin 2\vartheta \rangle & -\frac{a}{2}\langle \sin \phi \sin 2\vartheta \rangle & \frac{\sigma_{\perp} + \sigma_{\parallel} + 4\sigma_e - a\langle \cos 2\vartheta \rangle}{2} \end{pmatrix}. \quad (A7)$$

If the conductivity axes of all cells are oriented in the direction of the applied field \mathbf{E} (in z -direction), then the effective conductivity is diagonal ($\sigma_{i \neq j} = 0$):

$$\sigma = \begin{pmatrix} \sigma_e + 3f\sigma_e \frac{3f\sigma_e(\sigma_{\perp} - \sigma_e)}{(\sigma_{\perp} - \sigma_e)(1-f) + 3\sigma_e} & 0 & 0 \\ 0 & \sigma_e + 3f\sigma_e \frac{3f\sigma_e(\sigma_{\perp} - \sigma_e)}{(\sigma_{\perp} - \sigma_e)(1-f) + 3\sigma_e} & 0 \\ 0 & 0 & \sigma_e + 3f\sigma_e \frac{3f\sigma_e(\sigma_{\parallel} - \sigma_e)}{(\sigma_{\parallel} - \sigma_e)(1-f) + 3\sigma_e} \end{pmatrix}. \quad (A8)$$

The tensor has uniaxial symmetry, and its diagonal elements are given by the Maxwell equation for isotropic particles having $\sigma_p = \sigma_{\perp}$ and $\sigma_p = \sigma_{\parallel}$.

If the conductivity axes of all cells are oriented in the y -direction (perpendicular to the applied electric field), then the effective conductivity is again diagonal ($\sigma_{i \neq j} = 0$),

$$\begin{aligned} \sigma_{11} = \sigma_{33} &= \sigma_e + 3f\sigma_e \frac{(\sigma_{\perp} - \sigma_e)}{(\sigma_{\perp} - \sigma_e)(1-f) + 3\sigma_e}, \\ \sigma_{22} &= \sigma_e + 3f\sigma_e \frac{(\sigma_{\parallel} - \sigma_e)}{(\sigma_{\parallel} - \sigma_e)(1-f) + 3\sigma_e}. \end{aligned} \quad (A9)$$

For uniform orientation distribution over all angles is the effective conductivity isotropic:

$$\sigma = \sigma_e + 3f\sigma_e \frac{(\sigma_{\perp} + 2\sigma_e)(\sigma_{\parallel} - \sigma_e) - 2\sigma_e(\sigma_{\parallel} - \sigma_{\perp})}{(1-f)(\sigma_{\perp} + 2\sigma_e)(\sigma_{\parallel} + 2\sigma_e) + f\sigma_e(\sigma_{\perp} + 2\sigma_{\parallel} + 6\sigma_e)}. \quad (A10)$$

This is a Maxwell approximation for randomly oriented anisotropic particles (cells) embedded in an isotropic medium.

For cells in a suspension, it is realistic to assume that we have a uniform distribution over angles ϕ and a normal distribution over the angles ϑ around angle $\vartheta = 0$,

$$\Gamma(z) = \frac{1}{\gamma\sqrt{2\pi}} e^{-\frac{(z-1)^2}{2\gamma^2}}, \quad (A11)$$

where $z = \cos \vartheta$ and γ is the width of the distribution. For larger interactions between the cells, the cells rotate more, so parameter γ is larger. However, we have to also take into account that normal distribution is defined on an infinite interval, whereas z goes only from -1 to 1 ($\vartheta = [0, \pi]$). Thus, the assumption of the normal distribution is physically valid only for the distribution which is narrow enough, so that the part of the distribution tail for z below -1 can be neglected; i.e., $\Gamma(z = 1) \ll \Gamma(z = 0)$. To calculate

the effective conductivity of the cells which have such a distribution, we first have to calculate the matrices A and B and all the averages over angles for this distribution. Since all nondiagonal elements are zero for a uniform

distribution over ϕ , we have to calculate only the following averages:

$$\begin{aligned} \langle \cos^2 \vartheta + \sin^2 \phi \sin^2 \vartheta \rangle &= \frac{1}{4\pi} \int_0^{2\pi} d\phi \int_{-1}^1 [z^2 + \sin^2 \phi (1 - z^2)] \Gamma(z) dz \\ &= \frac{5}{16} - \frac{\gamma^2}{2}, \end{aligned} \quad (A12)$$

$$\langle \cos 2\vartheta \rangle = \frac{1}{4\pi} \int_0^{2\pi} d\phi \int_{-1}^1 [2z^2 - 1] \Gamma(z) dz = \frac{1}{2} - 2\gamma^2. \quad (A13)$$

From this, we obtain third diagonal component of the effective conductivity tensor,

$$\sigma_{33} = \sigma_e + 3f\sigma_e \frac{A_{33}}{(1-f)(\sigma_{\perp} + 2\sigma_e)(\sigma_{\parallel} + 2\sigma_e) + 3f\sigma_e B_{33}}, \quad (A14)$$

where

$$\begin{aligned} A_{33} &= b + \frac{3a\sigma_e}{2} \left[-2\gamma^2 - \frac{1}{2} \right], \\ B_{33} &= \frac{\sigma_{\perp} + \sigma_{\parallel} + 4\sigma_e - a \left[\frac{1}{2} - 2\gamma^2 \right]}{2}. \end{aligned} \quad (A15)$$

With Eq. A14, it is thus possible to calculate the conductivity in the direction of the applied field for a given width γ of a normal distribution.

APPENDIX B

Here we reproduce the calculation of Hibino et al. (1991) of a membrane potential for a spherical cell with a finite membrane conductance placed in a homogeneous electric field. We deal only with a steady state. The electric potentials inside and outside the cell, ψ_i and ψ_e , satisfy Laplace's equation,

$$\Delta\psi_i(r, \theta, \phi) = \Delta\psi_e(r, \theta, \phi) = 0, \quad (\text{B1})$$

with boundary conditions,

$$\sigma_i \left[\frac{\partial \psi_i}{\partial r} \right]_{r=R} = \sigma_e \left[\frac{\partial \psi_e}{\partial r} \right]_{r=R} = G[\psi_e - \psi_i]_{r=R}, \quad (\text{B2})$$

$$\lim_{R \rightarrow \infty} \psi_e \rightarrow E_0 R \cos \theta$$

where E_0 is the intensity of the electric field far from the cell; σ_i and σ_e are the conductivities of the inter- and extracellular medium, respectively; R is the cell radius; G is the membrane conductance; and (r, θ, ϕ) are the polar coordinates. We introduce dimensionless quantities:

$$\Psi_i = \frac{\psi_i}{RE_0}, \quad \Psi_e = \frac{\psi_e}{RE_0}, \quad r' = r/R, \\ \nu = \sigma_i/\sigma_e, \quad \text{and} \quad g(\theta) = R/\sigma_i G(\theta), \quad (\text{B3})$$

where $g(\theta)$ represents normalized conductance of the membrane:

$$g(\theta) = \begin{cases} g_0 \frac{(|\cos \theta| - \cos \theta_c)^j}{(1 - \cos \theta_c)^j} & |\cos \theta| > \cos \theta_c \\ 0 & |\cos \theta| \leq \cos \theta_c \end{cases} \quad (\text{B4})$$

If we assume that $g(\theta)$ is symmetric around the z -axis, then Ψ values are also symmetric around the z -axis. The solution of Eqs. B1 and B2 can be written as

$$\Psi_i = c_0 + \sum_{n=1}^{\infty} \frac{c_n (r')^n P_n(\cos \theta)}{n}, \quad (\text{B5})$$

$$\Psi_e = \left[r' + \frac{1}{2r'^2} \right] P_1(\cos \theta) + \nu \sum_{n=1}^{\infty} \frac{c_n P_n(\cos \theta)}{(n+1)(r')^{n+1}}, \quad (\text{B6})$$

where P_n is the Legendre polynomial of order n , and c_n values are constants. Under assumed symmetry, only odd c_n values are nonzero. By introduction of Eqs. B4–B6 into Eq. B2, and by using the orthogonality of Legendre's polynomials, we obtain

$$\frac{2}{2m+1} c_m = \frac{3}{2} g_{m1} - \sum_{n=1}^{\infty} c_n \left[\frac{1}{n} + \frac{\nu}{n+1} \right] g_{nm}, \quad (\text{B7})$$

where g_{nm} are the elements of the $n \times m$ matrix of the integrals,

$$g_{nm} = \int_0^\pi P_m(\cos \vartheta) g(\vartheta) P_n(\cos \vartheta) d(\cos \vartheta). \quad (\text{B8})$$

For $m = 1, \dots, \infty$, Eq. B7 constitutes a linear equation system for c_n values. For finite N , we obtain a finite system of linear equations for coefficient c_n values.

Authors thank Francis X. Hart from the University of the South, Sewanee, Tennessee, for his valuable suggestions and comments during the

preparation of the manuscript. M.P. also thanks Vladimir B. Bregar for his invaluable contribution to this manuscript.

This research was in part supported by the Ministry of Education, Science and Sports of the Republic of Slovenia, and the European Commission, under the grant Cliniporator QLK3-99-00484 within the 5th framework.

REFERENCES

- Abidor, I. G., A. I. Barbul, D. V. Zhelev, P. Doinov, I. N. Bandarina, E. M. Osipova, and S. I. Sukharev. 1993. Electrical properties of cell pellet and cell fusion in a centrifuge. *Biochim. Biophys. Acta.* 152:207–218.
- Abidor, I. G., L.-H. Li, and S. W. Hui. 1994. Studies of cell pellets. II. Osmotic properties, electroporation, and related phenomena: membrane interactions. *Biophys. J.* 67:427–435.
- Davalos, R. V., Y. Huang, and B. Rubinsky. 2000. Electroporation: bio-electrochemical mass transfer at the nano scale. *Microscale Thermophys. Eng.* 4:147–159.
- Davalos, R. V., B. Rubinsky, and D. M. Otten. 2002. A feasibility study for electrical impedance tomography as a means to monitor tissue electroporation for molecular medicine biomedical engineering. *IEEE Tran. Biomed. Eng.* 49:400–403.
- DeBruin, K. A., and W. Krassowska. 1999a. Modeling electroporation in a single cell. I. Effects of field strength and rest potential. *Biophys. J.* 77:1213–1223.
- DeBruin, K. A., and W. Krassowska. 1999b. Modeling electroporation in a single cell. II. Effects of ionic concentrations. *Biophys. J.* 77:1225–1233.
- Dukhin, S. S. 1971. Dielectric properties of disperse systems. In *Surface and Colloid Science*, Vol. 3. E. Matijević, editor. Wiley-Interscience, New York. pp.83–165.
- Foster, K. R., and H. P. Schwan. 1986. Dielectric properties of tissues. In *Handbook of Biological Effects of Electromagnetics Fields*. C. Polk and E. Postow, editors. CRC Press, Florida. pp.28–96.
- Gabriel, B., and J. Teissie. 1997. Direct observation in the millisecond time range of fluorescent molecule asymmetrical interaction with the electropermeabilized cell membrane. *Biophys. J.* 73:2630–2637.
- Gabriel, B., and J. Teissie. 1998. Fluorescence imaging in the millisecond time range of membrane electropermeabilization of single cells using a rapid ultra-low-light intensifying detection system. *Eur. Biophys. J.* 27:291–298.
- Hibino, M., M. Shigemori, H. Itoh, K. Nagayama, and K. Kinoshita, Jr. 1991. Membrane conductance of an electroporated cell analyzed by submicrosecond imaging of transmembrane potential. *Biophys. J.* 59:209–220.
- Hibino, M., H. Itoh, and K. Kinoshita, Jr. 1993. Time courses of cell electroporation as revealed by submicrosecond imaging of transmembrane potential. *Biophys. J.* 64:1789–1800.
- Jarozeski, M. J., R. Heller, and R. Gilbert. 1999. *Electrochemotherapy, Electrogenotherapy and Transdermal Drug Delivery: Electrically Mediated Delivery of Molecules to Cells*. Humana Press, New Jersey.
- Kinoshita, K., and T. Y. Tsong. 1979. Voltage-induced conductance in human erythrocyte. *Biochim. Biophys. Acta.* 554:479–497.
- Kotnik, T., F. Bobanović, and D. Miklavčič. 1997. Sensitivity of transmembrane voltage induced by applied electric fields—a theoretical analysis. *Bioelectrochem. Bioenerg.* 43:285–291.
- Levy, O., and D. Stroud. 1997. Maxwell Garnett theory for mixtures of anisotropic inclusions: application to conducting polymers. *Phys. Rev. B.* 56:8035–8042.
- Maxwell, J. C. 1873. *Treatise on Electricity and Magnetism*. Oxford University Press, London, UK.
- Miklavčič, D., D. Šemrov, H. Mekid, and L. M. Mir. 2000. A validated model of in vivo electric field distribution in tissues for electro-

- chemotherapy and for DNA electrotransfer for gene therapy. *Biochim. Biophys. Acta*. 1519:73–83.
- Mir, L. M. 2000. Therapeutic perspectives of in vivo cell electro-permeabilization. *Bioelectrochemistry*. 53:1–10.
- Neumann, E., M. Schaefer-Ridder, Y. Wang, and P. H. Hofschneider. 1982. Gene transfer into mouse lyoma cells by electroporation in high electric fields. *EMBO J.* 1:841–845.
- Neumann, E., A. E. Sowers, and C. A. Jordan. 1989. Electroporation and electrofusion in cell biology. Plenum Press, New York.
- Pauly, V. H., and H. P. Schwan. 1959. Über die impedanz einer suspension von kugelförmigen teilchen mit einer schale. *Z. Naturforsch.* 14b:125–131.
- Pavlin, M., T. Slivnik, and D. Miklavčič. 2002a. Effective conductivity of cell suspensions. *IEEE Tran. Biomed. Eng.* 49:77–80.
- Pavlin, M., N. Pavšelj, and D. Miklavčič. 2002b. Dependence of induced transmembrane potential on cell density, arrangement and cell position inside a cell system. *IEEE Tran. Biomed. Eng.* 49:605–612.
- Ryttsen, F., C. Farre, C. Brennan, S. G. Weber, K. Nolkranz, K. Jardemark, D. T. Chiu, and O. Orwar. 2000. Characterization of single-cell electroporation by using patch-clamp and fluorescence microscopy. *Biophys. J.* 79:1993–2001.
- Sukharev, S. I., V. A. Klenchin, S. M. Serov, L. V. Chernomordik, and Y. A. Chizmadzhev. 1992. Electroporation and electrophoretic DNA transfer into cells. The effect of DNA interaction with electropores. *Biophys. J.* 63:1320–1327.
- Susil, R., D. Šemrov, and D. Miklavčič. 1998. Electric field-induced transmembrane potential depends on cell density and organization. *Electro. Magnetobiol.* 17:391–399.
- Serša, G., T. Čufer, M. Čemazar, M. Reberšek, and Z. Rudolf. 2000. Electrochemotherapy with bleomycin in the treatment of hypernephroma metastasis: case report and literature review. *Tumori*. 86:163–165.
- Šemrov, D., and D. Miklavčič. 1999. Numerical modelling for in vivo electroporation. In *Electrochemotherapy, Electrogenetherapy and Transdermal Drug Delivery: Electrically Mediated Delivery of Molecules to Cells*. M. J. Jaroszeski, R. Heller, and R. Gilbert, editors. Humana Press, New Jersey. pp.63–81.
- Teissie, J., and M. P. Rols. 1993. An experimental evaluation of the critical potential difference inducing cell membrane electropermeabilization. *Biophys. J.* 65:409–413.
- Takashima, S. 1989. Electrical Properties of Biopolymers and Membranes. Adam-Hilger, Bristol, UK.
- Tekle, E., R. D. Astumian, and P. B. Chock. 1990. Electro-permeabilization of cell membranes: effect of the resting membrane potential. *Biochem. Biophys. Res.* 172:282–287.
- Tsong, T. Y. 1991. Electroporation of cell membranes. *Biophys. J.* 60:297–306.
- Valič, B., M. Golizio, M. Pavlin, A. Schatz, B. Gabriel, J. Teissie, M. Rols, and D. Miklavčič. 2003. Electric field induced transmembrane potential on spheroidal cell: theory and experiment. *Eur. Biophys. J.*
- Weaver, J. C., and Y. A. Chizmadzhev. 1996. Theory of electroporation: a review. *Bioelectrochem. Bioenerg.* 41:135–160.
- Zimmermann, U. 1982. Electric field-mediated fusion and related electrical phenomena. *Biochim. Biophys. Acta*. 694:227–277.
- Zimmermann, U. 1996. The effect of high-intensity electric field pulses on eukaryotic cell membranes: fundamentals and applications. In *Electromanipulation of Cells*. U. Zimmermann, and G. A. Neil, editors. CRC Press, London, UK. pp.1–105.